

Primljen / Received: 3.9.2021.

Ispravljen / Corrected: 13.7.2022.

Prihvaćen / Accepted: 1.2.2023.

Dostupno online / Available online: 10.6.2023.

A site survey of damaged RC buildings in İzmir after the Aegean sea earthquake on October 30, 2020

Authors:



Assist.Prof. **Halit Cenan Mertol**, PhD. CE
Atılım University, Ankara, Turkey
Department of Civil Engineering
cenan.mertol@atilim.edu.tr

Corresponding author



Assist.Prof. **Gokhan Tunc**, PhD. CE
Atılım University, Ankara, Turkey
Department of Civil Engineering
gokhan.tunc@atilim.edu.tr



Prof. **Tolga Akis**, PhD. CE
Atılım University, Ankara, Turkey
Department of Civil Engineering
tolga.akis@atilim.edu.tr

Research Paper

Halit Cenan Mertol, Gokhan Tunc, Tolga Akis

A site survey of damaged RC buildings in İzmir after the Aegean sea earthquake on October 30, 2020

An earthquake with a magnitude of $M_w = 6.6$ and a depth of approximately 16.5 km occurred on 30 October 2020 off the coast of Samos, a Greek island 35 km southwest of Seferihisar, a town in İzmir. The earthquake caused several collapses and severe structural damage in approximately 6,000 buildings, specifically in the Bayraklı District in İzmir Bay. This paper presents the observations and findings of a technical team that visited the earthquake-affected areas immediately after the earthquake. Eleven partially or fully collapsed and several severely damaged reinforced concrete buildings were investigated. Based on the site investigations, we observed that almost all of the collapsed or severely damaged reinforced concrete buildings in the region were built between 1975 and 2000. Site observations also confirmed that the construction of these collapsed or damaged buildings did not conform to the requirements outlined in the Turkish Earthquake Codes used at the time. The failures and severe damage to buildings in earthquake-affected areas are primarily related to inadequate reinforcement configuration, poor material quality, the absence of geotechnical studies, and framing problems related to their lateral load-carrying systems. Therefore, it is recommended that all the buildings located in and around İzmir Bay, particularly those built between 1975 and 2000, be structurally evaluated to prevent any further loss of life and property during future earthquakes.

Key words:

structural failure, reinforced concrete buildings, 2020 Aegean Sea earthquake, İzmir

Prethodno priopćenje

Halit Cenan Mertol, Gokhan Tunc, Tolga Akis

Oštećenja AB zgrada u İzmiru nakon potresa u Egejskom moru 30. listopada 2020.

Potres magnitude $M_w = 6,6$ i dubine od približno 16,5 km dogodio se 30. listopada 2020. uz obalu grčkog otoka Samosa, 35 km jugozapadno od grada Seferihisara u İzmiru. Potres je prouzročio nekoliko urušavanja i teška oštećenja približno 6000 zgrada, posebice onih u četvrti Bayraklı u Izmirskom zaljevu. U radu su prikazana zapažanja i nalazi tehničkog tima koji je neposredno nakon potresa obišao potresom pogođena područja. Istraženo je jedanaest djelomično ili potpuno urušenih zgrada i nekoliko teško oštećenih armiranobetonskih zgrada. Na temelju zapažanja na mjestu događaja, uočeno je da su gotovo sve urušene ili teško oštećene armiranobetonske zgrade u regiji izgrađene u periodu između 1975. i 2000. godine. Promatranja su također potvrdila da gradnja tih urušenih ili oštećenih zgrada nije bila u skladu sa zahtjevima navedenima u turskim potresnim normama koje su se tada primjenjivale. Otkazivanja konstrukcija i teška oštećenja zgrada u potresom pogođenim područjima prije svega su povezana s neadekvatnim oblikovanjem armature, lošom kvalitetom materijala, nedostatkom geotehničkih istraživanja i problemima ostvarivanja okvira kao bočnih nosivih sustava. Stoga se preporučuje da se nosiva konstrukcija svih zgrada koje se nalaze u Izmirskom zaljevu i oko njega, posebno onih izgrađenih između 1975. i 2000., procijeni kako bi se spriječio daljnji gubitak života i imovine tijekom budućih potresa.

Ključne riječi:

otkazivanje konstrukcije, armiranobetonske zgrade, potres u Egejskom moru 2020., İzmir

1. Introduction

Turkey lies in one of the most active earthquake zones worldwide. Based on statistical studies, in Turkey, a strong earthquake with a magnitude of M_w between 6.0 and 6.9 occurs every two years, and a major earthquake with a magnitude M_w of above 6.9 occurs every three years. Approximately 98 % of the Turkish population lives in earthquake-risk-designated areas. Since the establishment of the Turkish Republic in 1923, approximately 80,000 people have lost their lives owing to earthquakes. The total approximate direct and indirect costs of earthquake damage between 1980 and 2022 were estimated to be USD 40 billion [1, 2].

Turkey has several fault lines that can generate strong earthquakes. These include the North Anatolian Fault Line (NAF) and East Anatolian Fault Line (EAF) (Figure 1, adapted from Turkish General Directorate of Mineral Research and Exploration, MTA [3]). The western part of the country has several fault line segments with the potential to generate strong earthquakes. These fault lines can all be categorised under the West Anatolian Fault Line (WAF) (Figure 1). The NAF in northern Turkey extends close to 1,500 km and spans from east to west. In eastern and southeastern parts of the country, the EAF extends from the Gulf of Iskenderun to the city of Hakkari in the shape of an arc. In the western part of the country, the WAF covers an area of approximately 45,000 km² (almost 6 % of Turkey's total land area).

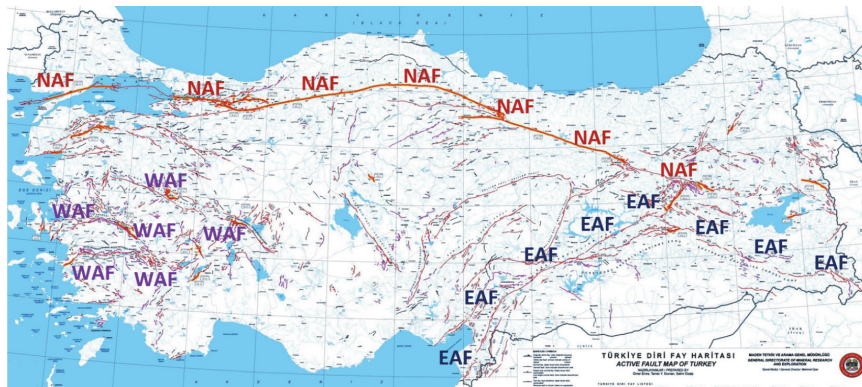


Figure 1. Turkey's active fault lines [3]



Figure 2. Location of the Aegean Sea earthquake (October 30, 2020)

Bayraklı, İzmir, located in the western part of Turkey, suffered a strong earthquake with a magnitude of $M_w = 6.6$ on 30 October 2020 [4]. The hypocentre was located 16.5 km below the epicentre. The earthquake affected more than four million people, living primarily in the city of İzmir and surrounding towns and villages, as well as the residents of Samos Island, Greece. The focus of this article is on the reinforced concrete (RC) buildings located in and around İzmir; therefore, the structural damage observed in Samos are not included in this study.

İzmir is the third most populated city in Turkey, with a total of population of nearly 4.4 million people. It also has the third highest gross domestic product (GDP) in the country, at 6.3 % of the total GDP [5]. The city centre is located approximately 67 km northeast of the epicentre of the earthquake, as shown in Figure 2. According to government data, 117 people lost their lives and approximately 32,000 people were injured owing to the earthquake. The earthquake caused the collapse of 11 RC buildings immediately after the main shock. According to detailed site investigations conducted by the government, close to 6,000 buildings experienced moderate-to-minor damage. Of these buildings, 511 had moderate damage, and 5,119 had minor damage. More than 500 buildings were structurally inadequate and were demolished [6].

Several scientific studies were conducted on the 2020 Aegean Sea earthquake. While some studies focused on the geotechnical and seismic aspects of earthquake [7-10], others focused on building damage [11-14]. The total direct cost of the earthquake damage was estimated to be approximately USD 400 million [15].

It is important to visually record earthquake-induced damage at a site immediately after an earthquake. This can provide valuable information to experts before structural demolitions and alterations occur. A reconnaissance team performed a technical visit to the earthquake-affected region within 24 h of the earthquake. This paper, which details the observations and outcomes of this site visit, adds to the current literature on the 2020 Aegean Sea earthquake by providing valuable onsite information on the seismic characteristics of the earthquake. These characteristics are based on data extracted from various strong ground motion stations, beginning from the closest Turkish station near the epicentre to the Bayraklı District where some RC buildings collapsed and others experienced moderate-to-major damage. The observations and findings of this site visit with respect to RC buildings are presented in this paper.

2. Seismicity and tectonics

2.1. History

During the Neotectonic Age (approximately 12 million years BC), plate movement began in the north–south direction due to the collision of the larger Arabian and smaller Anatolian plates [16] (Figure 3). Because of the collision between the Arabian and Anatolian plates, the western part of Anatolia moves at a speed of 40 mm/year in a counter-clockwise direction [17]. There are two important large-scale grabens (Gediz-GG and Büyükmenderes-BMG) in the regions with normal faulting mechanisms [18]. Both are young geological structures formed during the neotectonism of Western Anatolia and have the potential to generate destructive earthquakes. According to geological studies conducted in this region, strike-slip faulting mechanisms have been identified between these two important grabens in the N-S, NW-SE, and NE-SW directions [19–21].

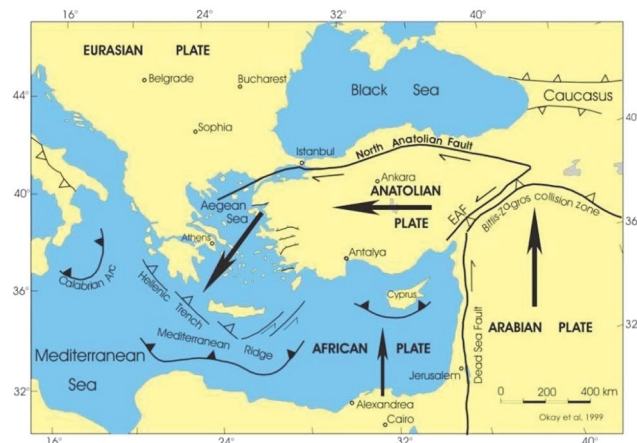


Figure 3. Intercontinental plate movement [16]

The seismicity in and around İzmir is generally governed by both normal and strike-slip fault mechanisms located between, and parallel to, the Büyük Menderes and Gediz grabens (Figure 4). These seismic activities are predominantly controlled by the İzmir, Tuzla, Karaburun, Yenifoça, Manisa, Kemalpaşa, Seferihisar, Menemen, Gülbahçe, and Dağkızılca fault lines as well as the Gediz Graben detachment fault [22]. The İzmir and Manisa fault lines, which exist to the south and east of the İzmir Bay area, are both governed by normal faults. This region also contains the Tuzla and Yenifoça faults, whose strike-slip mechanisms are located in the northeast–southwest direction of the bay area [23]. The formation of İzmir Bay began through normal faults that occurred during the Early Pliocene in the western part of Turkey [24, 25]. In the Late Quaternary, early delta progradation of sediments occurred in the bay area [26]. Therefore, the local geology of the coastline of the İzmir Bay area consists of Quaternary alluvium surrounded by a Paleocene flysch zone (limestones) and Miocene sandstones/mudstones [27–29]. The depth to bedrock in the bay area varies from 900 to 1,200 m, and the groundwater level is between 1.0 and 10.0 m [30, 31].



Figure 4. Active fault lines in the İzmir area [3, 22]

2.2. Earthquake hazard map

The Earthquake Hazard Map of Turkey, which was prepared based on earthquakes with a 10 % exceedance probability in 50 years, or the equivalent of a return period of 475 years, is shown in Figure 5 [32].

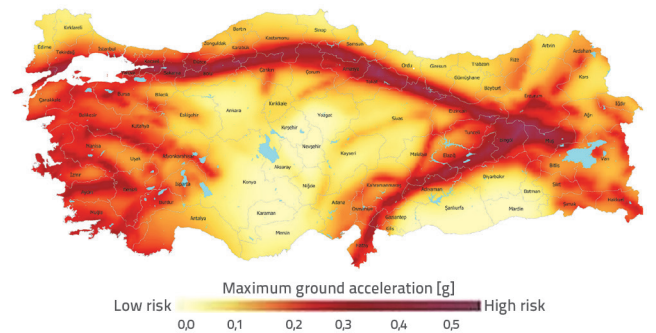


Figure 5. Earthquake Hazard Map of Turkey (return period of 475 years) [32]

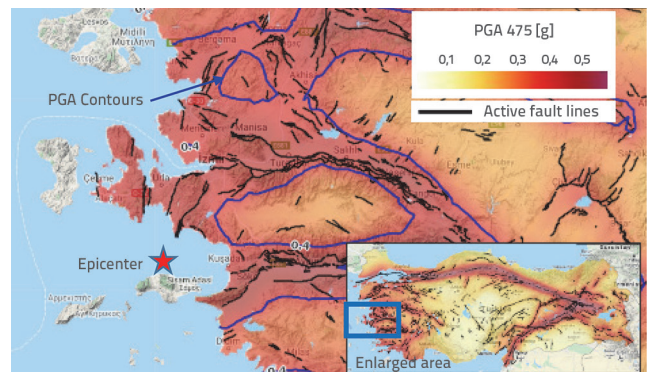


Figure 6. Expected peak ground acceleration values (in g) for earthquakes with a return period of 475 years in the western part of Turkey [32]

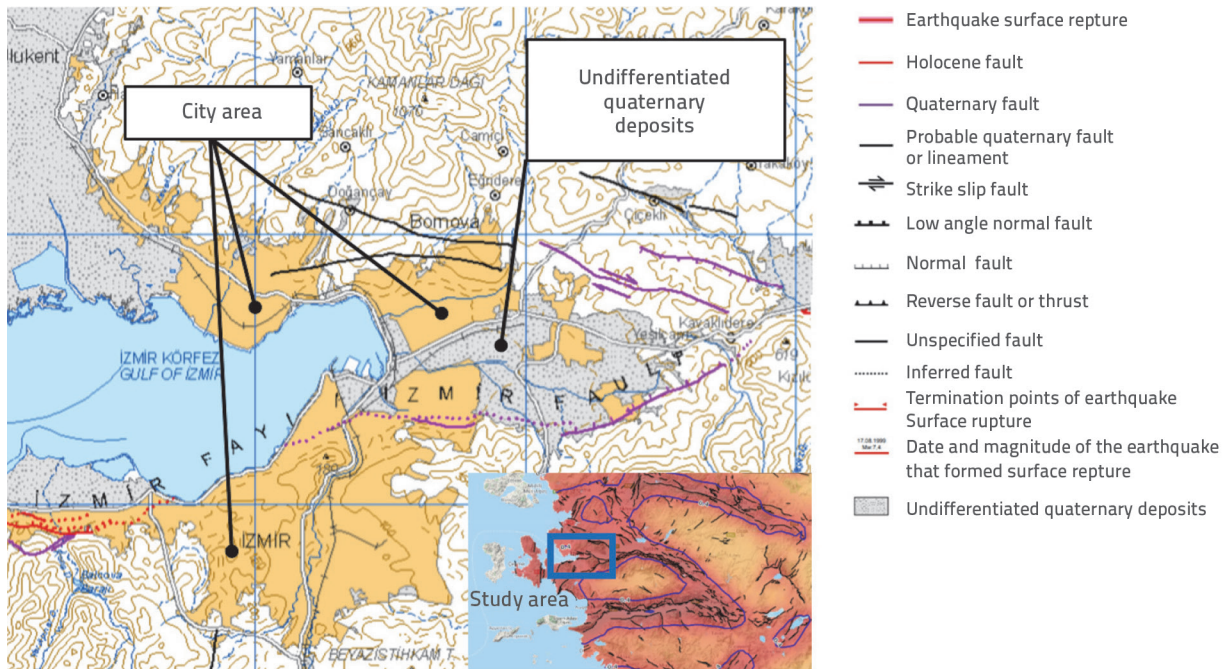


Figure 7. Active fault lines and general soil type in the İzmir Bay area [3]

Based on the peak ground accelerations shown in the map, the most severe earthquake regions are the northern, eastern, and southeastern parts of Turkey, including the area near the Aegean Sea, the inner southwestern part of Turkey, and the area around Lake Van. Figure 6 shows a more detailed hazard map of western Turkey, with the expected peak ground motion acceleration values calculated based on the same return period of 475 years, along with active fault lines [32]. Based on the data in Figure 6, the largest peak ground acceleration values in the region are approximately 0.4 g.

As this article focuses on the RC buildings located in the eastern part of İzmir Bay, it is important to emphasise the region's active fault lines and soil conditions. The map in Figure 7 shows the active fault lines and faulting mechanisms of the İzmir Bay area, including the dominant soil type [3]. Based on the map, the

dominant type of soil is undifferentiated Quaternary deposits. An in-depth discussion of soil types is provided in the next section.

2.3. Local soil conditions

Figure 8-a shows the aerial view of the İzmir Bay area and the region that experienced the most severe damage, which is shaded in blue. Figure 8-b provides information related to the detailed soil types in and around the bay area. According to the map, the dominant soil type of the bay area is undifferentiated Quaternary deposits, which is a type of soil that contains siliciclastic organics and freshwater carbonates. However, regions to the north, south, and west of the study area, each approximately 15 km away, have much better soil characteristics.

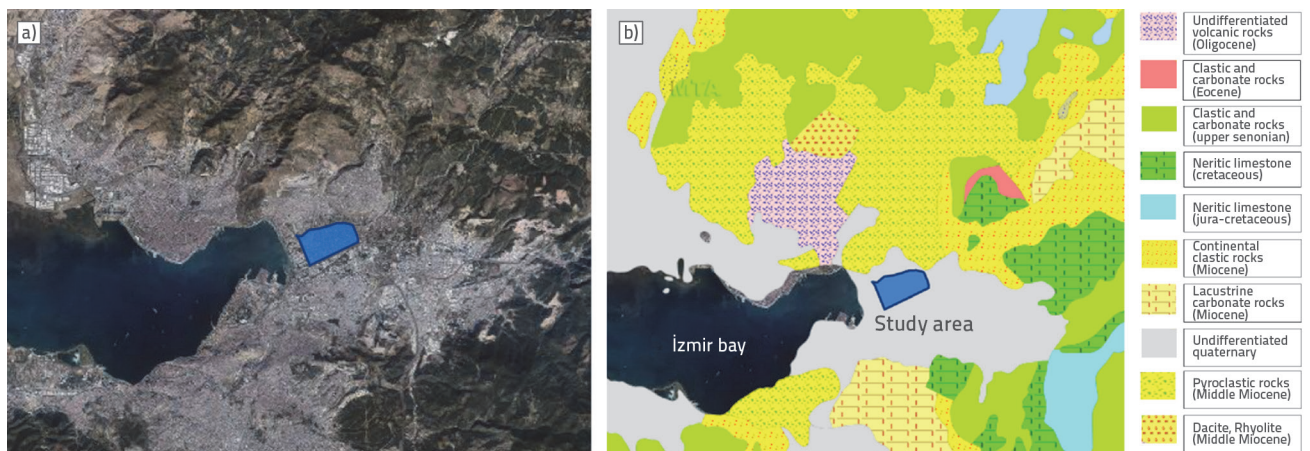


Figure 8. İzmir Bay area: a) aerial view; b) soil conditions [33]

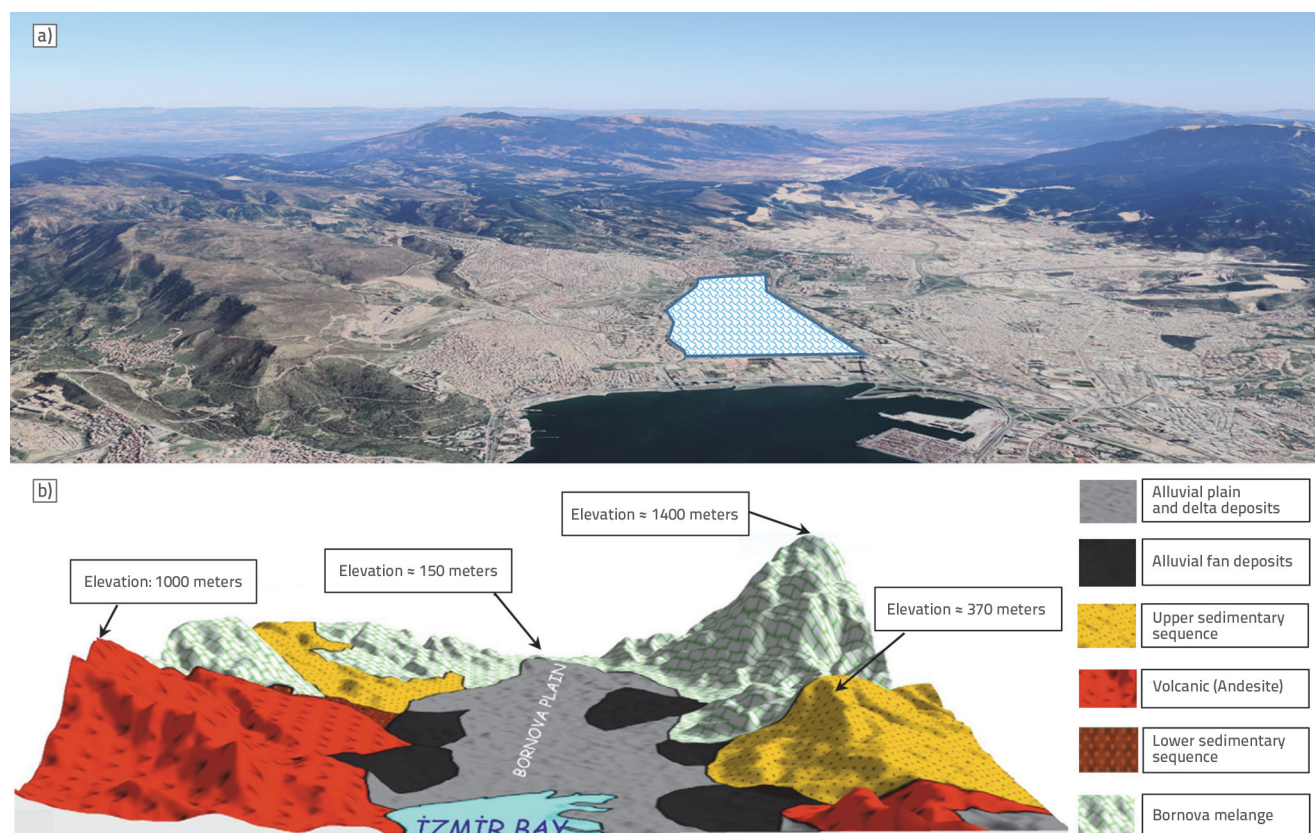


Figure 9. İzmir Bay area: a) 3D aerial view; b) soil conditions [34]

A 3D view of the study area and its soil conditions is shown in Figures 9-a and b. The soil conditions indicate that alluvial plain and delta deposits cover the entire study area and almost the entire bay area [34].

2.4. Aegean sea earthquake

The Aegean Sea earthquake occurred on 30 October 2020 at 14:51:23 local time [4]. The earthquake's epicentre was off the coast of Samos Island, Greece, which is located 35 km away from the southwestern part of the city of İzmir. The nearest inhabited Turkish town to the epicentre is the village of Payamlı. It is located in Seferihisar, a town in İzmir Province, which was 23.4 km away from the epicentre. The earthquake had a focal depth of 16.5 km and its magnitude was measured as $M_w = 6.6$

[4]. Table 1 lists the time, location, magnitude, and depth of the earthquake as recorded by different agencies.

The earthquake occurred due to normal faulting at a shallow crustal depth within the Eurasia tectonic plate of the eastern Aegean Sea. According to the USGS, the focal mechanism solution indicates that the earthquake occurred on a moderately dipping normal fault mechanism, indicating a north-south oriented extension, which is fairly common in the Aegean Sea [36]. Based on another study conducted by the MTA, an approximately 40 km long Samos fault line ruptured during the earthquake [39]. It was also stated that the strain energy probably shifted over to the western part of the Samos fault line, extending from the North-East to the South-West. The results from the moment tensor solution of the earthquake, as prepared by different agencies, are listed in Table 2.

Table 1. Characteristics of the Aegean Sea earthquake, 30 October, 2020

Source*	Local time	GPS coordinates	Magnitude	Depth [km]
AFAD [4]	14:51:23	37.879 N - 26.703 E	6.6 (M_w)	16.5
KOERI [35]	14:51:26	37.902 N - 26.794 E	6.9 (M_w)	12.0
USGS [36]	14:51:27	37.918 N - 26.790 E	7.0 (M_w)	21.0
CMT [37]	14:51:35	37.760 N - 26.680 E	7.0 (M_w)	12.0
GFZ [38]	14:51:27	37.900 N - 26.820 E	7.0 (M_w)	15.0

*AFAD: Disaster and Emergency Management Authority in Turkey; KOERI: Kandilli Observatory and Earthquake Research Institute; USGS: United States Geological Survey; CMT: Centroid-Moment-Tensor Project; GFZ: GeoForschungsZentrum, Germany

Table 2. Characteristic of the Aegean Sea earthquake, October 30, 2020

Source	Moment tensor	Strike 1	Dip 1	Rake 1	Strike 2	Dip 2	Rake 2
AFAD [4]		95	43	-87	270	46	-91
KOERI [35]		97	34	-85	272	55	-93
USGS [36]		93	61	-91	276	29	-88
CMT [37]		96	53	-86	270	37	-95
GFZ [38]		97	41	-85	272	48	-93

Historically, the İzmir region has been very active and has experienced numerous large magnitude earthquakes. Since 1900, a total of 695 earthquakes with magnitudes greater than or equal to 4.0 have been recorded during the instrumental period. Out of these 695 earthquakes, the largest magnitude was 6.8, which occurred in 1955. A total of 332 earthquakes were also recorded during the non-instrumental period, pre 1900 (Figure 10) [4, 35].

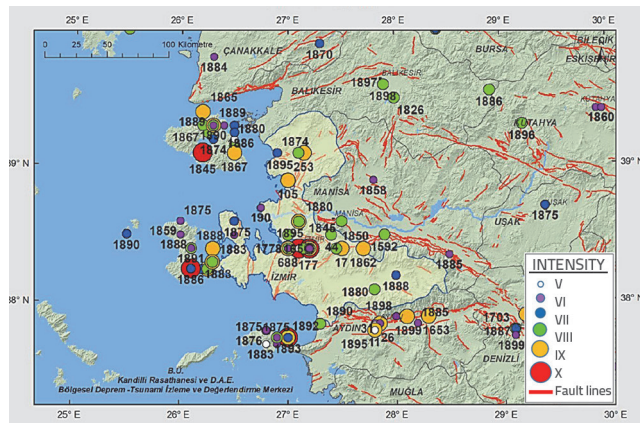


Figure 10. Pre 1900 earthquakes in and around İzmir (based on Mercalli Intensity Scale) [4, 35]

After the mainshock of the earthquake, a tsunami occurred in the region with a maximum wave height of 3.82 m [39]. The waves in the northern direction hit the shore of the Bay of Sığacık, a district in Seferihisar, and in the southern direction, on the northern shore of Samos Island [40]. Based on the authors' site observations, the waves moved as much as 200 to 250 m inland, into the district of Sığacık.

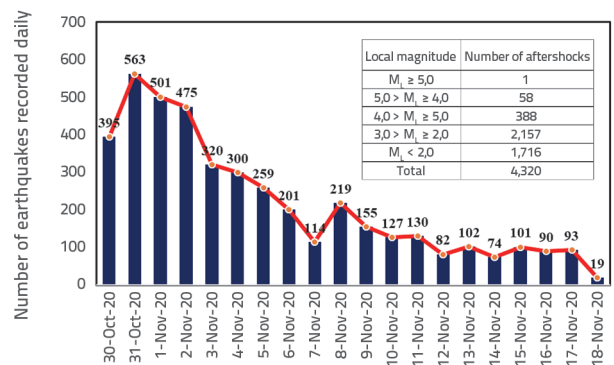


Figure 11. Total number of aftershocks recorded in the region between October 30, 2020 and November 18, 2020

According to the earthquake data collected between October 30, 2020 and November 18, 2020 (20 days), a total of 4,320

Table 3. Earthquake data extracted from the 16 strong ground motion recording stations

No	Station number	City	Town	Latitude [°]	Longitude [°]	Peak ground [Gal], Gal = 10 ⁻² m/s ²			R _{epi} [km]
						NS	EW	Vertical	
1	3536	İzmir	Seferihisar	38.1968	26.8384	50.220	79.139	31.315	34.745
2	0905	Aydın	Kuşadası	37.8560	27.2650	179.314	144.017	79.839	42.948
3	3523	İzmir	Urla	38.3282	26.7706	80.320	63.572	36.899	48.940
4	3533	İzmir	Menderes	38.2572	27.1302	73.635	45.899	37.460	51.380
5	3516	İzmir	Güzelbahçe	38.3706	26.8907	47.291	48.356	32.082	54.565
6	3538	İzmir	Gaziemir	38.3187	27.1234	85.484	76.953	39.264	56.665
7	3506	İzmir	Konak-1	38.3944	27.0821	43.879	41.039	23.587	62.304
8	3517	İzmir	Buca-1	38.3756	27.1936	40.099	36.136	19.816	65.316
9	3512	İzmir	Buca-2	38.4009	27.1516	57.541	56.746	28.158	65.761
10	3518	İzmir	Konak-2	38.4312	27.1435	106.103	91.449	31.143	68.365
11	3519	İzmir	Karşıyaka-1	38.4525	27.1112	150.089	109.975	34.173	69.225
12	3521	İzmir	Karşıyaka-2	38.4679	27.0764	110.844	93.986	40.312	69.581
13	3522	İzmir	Bornova-1	38.4357	27.1987	73.721	63.941	24.647	71.182
14	3513	İzmir	Bayraklı-1	38.4584	27.1671	106.281	94.667	44.186	72.002
15	3514	İzmir	Bayraklı-2	38.4762	27.1581	39.421	56.024	25.148	73.388
16	3520	İzmir	Bornova-2	38.4780	27.2111	36.112	58.549	19.367	75.777

aftershocks were recorded in the area, with local magnitudes varying from 0.8 to 5.2 [35]. Figure 11 shows the daily frequency distribution of these aftershock earthquakes. In order to determine the characteristics of the aftershocks, the total number of aftershocks is also categorized according to their magnitudes, as displayed in the figure.

Table 3 lists the peak ground acceleration values recorded by AFAD at the nearest sixteen strong ground motion stations [32]. The locations of these stations are plotted on the map in Figure 12. The station closest to the earthquake was the Seferihisar station (station number 3536), which was 35 km from the epicentre. The most distant station was Bornova station (station number 3520), which was 76 km from the epicentre. The maximum peak ground acceleration recorded at the Kuşadası station (station number 0905) was in the East direction with a magnitude of 0.179 g.

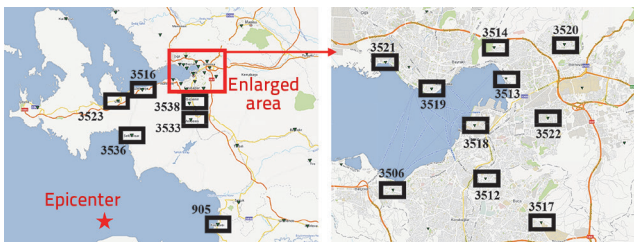


Figure 12. Locations of the 16 strong ground motion recording stations

2.5. Arias and housner intensities and spectral acceleration values of the aegean sea earthquake

Figure 13.a depicts the variation in the horizontal and vertical peak ground accelerations from the nearest station (Seferihisar station 3536) to the farthest station (Bornova station 3520). The figure shows a total of three peaks at the epicentral distances of 40 km (Kuşadası, station number 0905), 55 km (Urla and Güzelbahçe, station numbers 3523 and 3516), and 70 km (İzmir Bay area, including Bayraklı and Karşıyaka, station numbers 3513 and 3519), which were all associated with local site conditions. The acceleration peak at the epicentral distance of 70 km was much more pronounced than the other two peaks. This led to the immediate collapse of eleven buildings and severe structural damage in the Bayraklı district. Figure 13.b shows the variation in effective earthquake duration. Based on the data, the effective duration increased as the earthquake moved into the İzmir Bay area, leading to an increase from an average of 16 to 23 s in the horizontal directions. This increase was more prominent in the vertical component of the earthquake.

The variations in the Arias and Housner Intensities of the Aegean Sea earthquake are plotted in Figure 14.a and b in the N-S, E-W, and vertical directions based on the ground motion data recorded at 16 stations (Figure 12 for their locations). The data used in these figures clearly indicate that the intensity of the earthquake was greater in the regions around İzmir Bay, Bayraklı, and Karşıyaka.

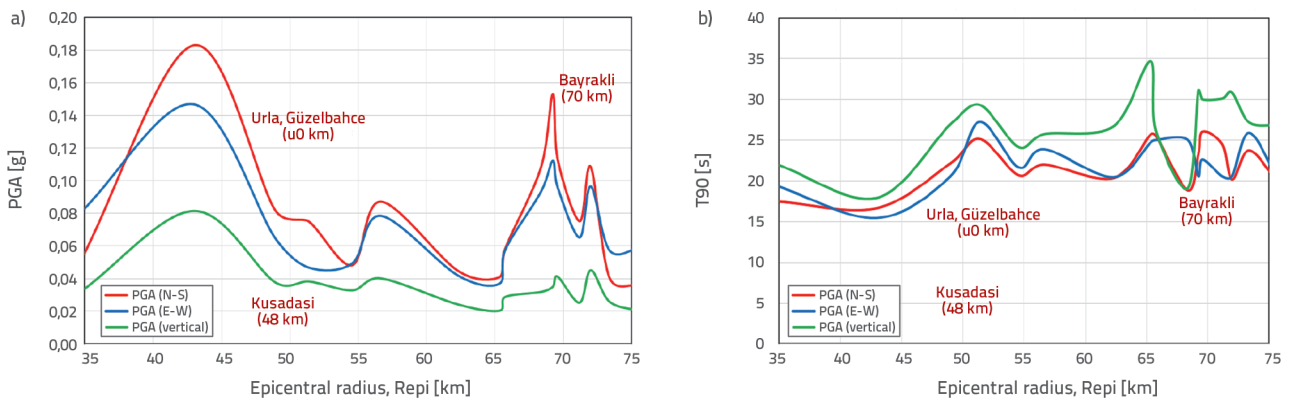


Figure 13. Aegean Sea Earthquake: a) PGA; b) effective duration

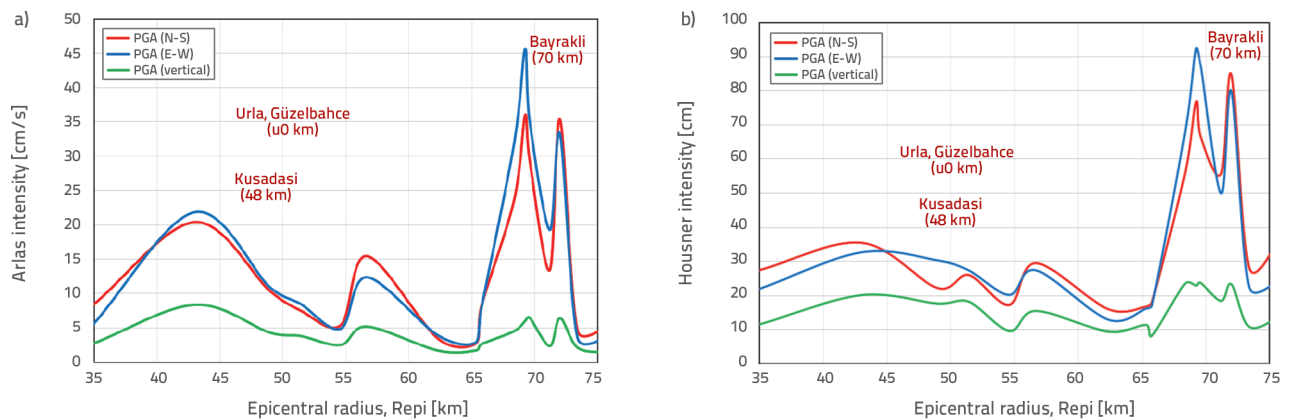


Figure 14. Aegean Sea earthquake: a) Arias intensity; b) Housner intensity

3. Evaluation of strong ground motion data

Strong ground-motion data were evaluated at six stations to better understand the impact and characteristics of the earthquake, specifically in the bay area (Figure 15). These stations are located along the earthquake route, starting from Kuşadası (station number 0905) to the station in the most affected area, Bayraklı (station number 3513), in the following order: 0905, 3536, 3518, 3513, 3519, and 3514. However, emphasis is given to the results extracted from the following three stations in and around the town of Bayraklı, which encircles the İzmir Bay area: 3513, 3518, and 3519.

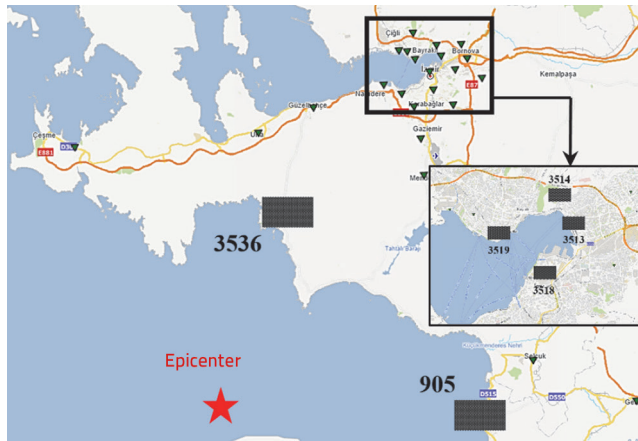


Figure 15. Locations of the six strong ground motion stations used to evaluate the Aegean Sea earthquake data

Figure 16 shows the peak ground acceleration values of the Aegean Sea earthquake in the north–south and east–west directions recorded at six stations. According to the data, the largest peak ground acceleration values were recorded at station number 0905 (located in the town of Kuşadası). The values at this station in both directions were 0.18g and 0.15g, respectively. The acceleration values are also provided in the Bayraklı area, where building collapses and severe structural damage were observed. The nearest station to Bayraklı is number 3513; it recorded 0.11g and 0.10g peak ground accelerations in the north–south and east–west directions, respectively.

The design spectrum curves of the current Turkish Building Earthquake Code (TBEC, 2018) [41] were compared with the measured spectral acceleration data, which were extracted from six stations in the north–south and east–west directions, as a function of varying damping ratios (Figure 16). TBEC (2018) [41] defined a total of six local soil classes, identified using letters from ZA through ZF, where ZA defines a hard rock soil type and ZF defines an extremely loose soil type, which requires further soil testing and site evaluation. In this study, the design spectrum curves of the first five soil classes (excluding soil type ZF) were used to evaluate the north–south and east–west peak ground acceleration components of the Aegean Sea earthquake. Based on the spectrum values, the peak ground acceleration values at stations 3536 and 3514 were much lower than the demands associated with the five soil classes. Therefore, the structural damage at these locations was moderate to minor. However, as the seismic waves travelled along stations

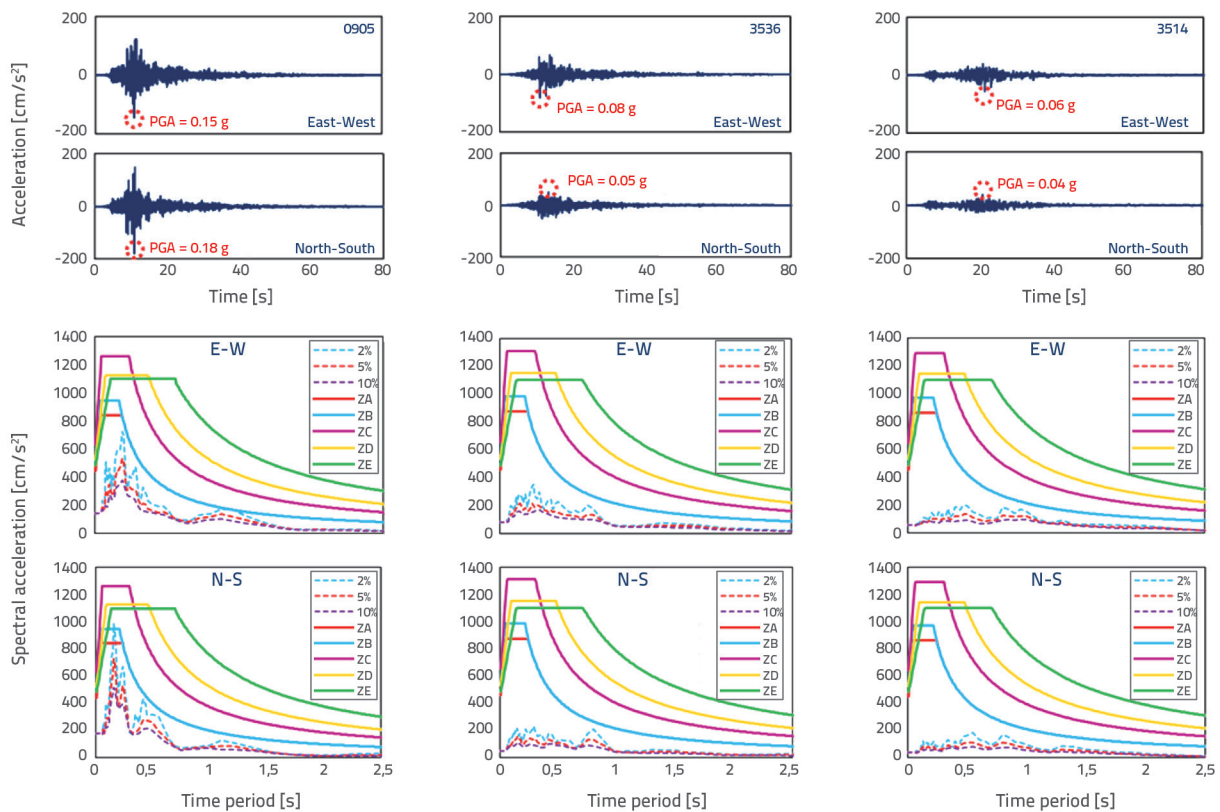


Figure 16. Peak ground and spectral acceleration values and design spectrum values for the Aegean Sea earthquake, 30 October, 2020 - Part I

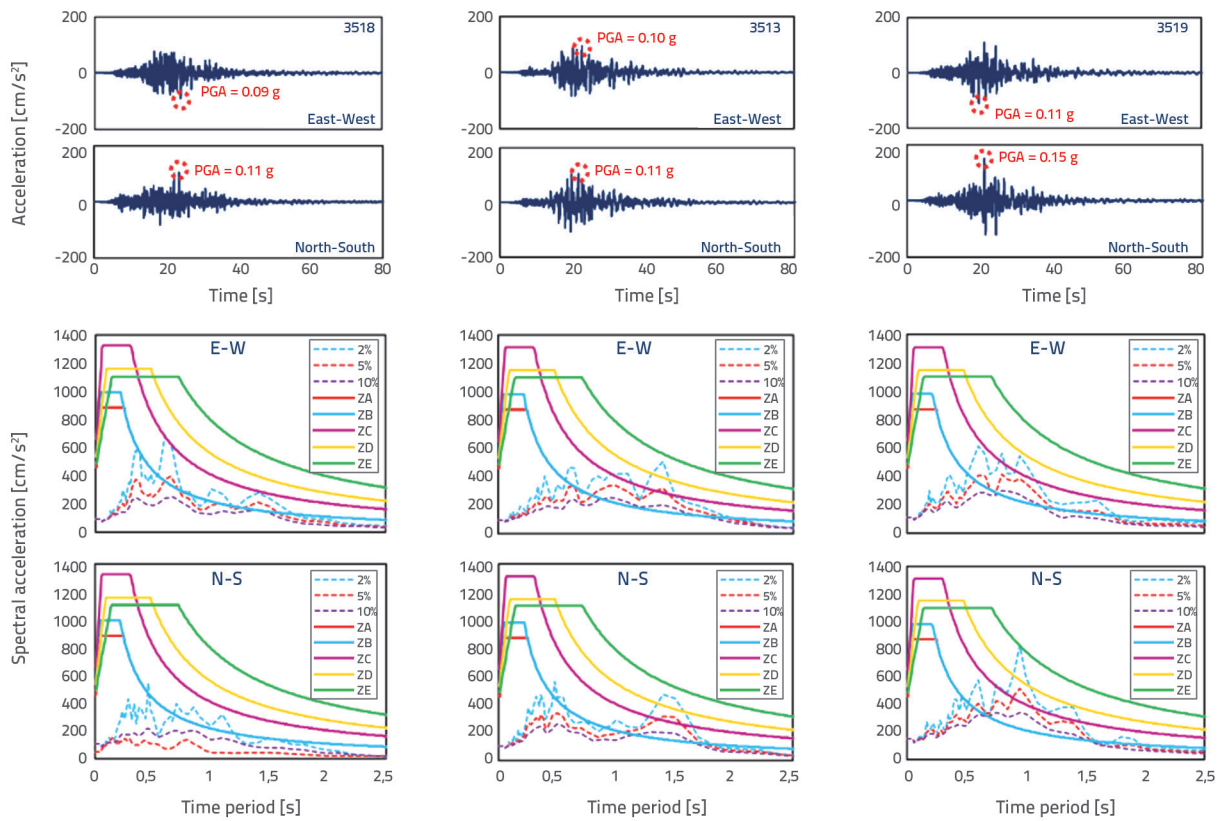


Figure 16. Peak ground and spectral acceleration values and design spectrum values for the Aegean Sea earthquake, 30 October, 2020 - Part II

0905, 3518, 3513, and 3519, the corresponding periods for the peak ground accelerations shifted from 0.2 to 1.5 s. This shift exceeded the code-generated design response spectrum values, specifically at stations 3513 and 3519, for all four soil types except for type ZE. As a result of this exceedance, the degree of structural damage varied from moderate to intense in RC buildings with 8–15 floors. To further evaluate the impact of the Aegean Sea earthquake, the local soil classes of the selected stations were considered. Figure 17 shows the soil classes at these stations [42].

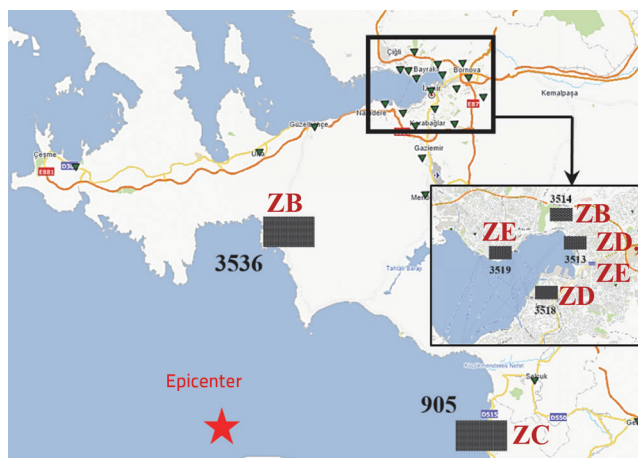


Figure 17. Local soil classes for the selected six stations

Based on this data, the soil properties of the Izmir Bay area appear to be the weakest because almost all the stations are located in soil classes ZD or ZE, which confirms the soil properties explained in Section 2.3. As expected, the weak soil amplified the peak ground acceleration and extended the effective duration by causing building collapse and severe structural damage. Although stations 3518 and 3519 both displayed acceleration patterns very similar to station 3513, the building damage near these two stations was not as severe as that at 3513. The severe building damage near station 3513 was largely attributed to the local soil type of the region (alluvial plain and delta deposits) (Figure 8.b). Another reason for this problem is the lack of geotechnical studies, which were not mandated at the time of construction (for further information, see Section 4.5.5).

4. Earthquake performance of reinforced concrete buildings

Building an effective framework for an extensive damage assessment of structures resulting from an earthquake is a very important concept for evaluating existing earthquake design codes and regulations. Many methods have been proposed by academic scholars in this field. Some of these methods are extremely detail-oriented and involve a resource-intensive process that requires full access to the structures in an earthquake-affected site, whereas

others are quicker and general and are often categorised under visual site inspections. A detailed evaluation of earthquake-induced damage was conducted separately for RC and masonry structures. The most frequently used structural damage evaluation systems are based on the European Macroseismic Scale (EMS-98), the Italian approach GNDT, and its US equivalent of the Applied Technology Council (ATC)-20 [43-45]. However, other methods are commonly used in Europe, such as the Greek Criteria [46], which were further elaborated based on extensive experience from past earthquakes [47]. This method has been used in other earthquake-prone countries such as Croatia [48].

In Turkey, the damage evaluation of RC buildings subjected to earthquakes is performed using the guidelines in [49] specified by the Turkish Chamber of Civil Engineers. Based on this document, the damage is classified into three groups: minor-, moderate-, and heavy. Minorly damaged buildings can be used immediately after an earthquake, moderately damaged buildings should be repaired and strengthened before occupation, and heavily damaged buildings should be demolished for economic reasons. The evaluation is performed in two stages (exterior and interior evaluation). If the building is partially or fully collapsed, the inter-story drift is greater than 0.02, or the building is tilted by more than 3°, the building is classified as heavily damaged. Interior evaluations are not conducted for these buildings. If the building is not classified as heavily damaged at the exterior evaluation stage, an interior evaluation is performed on the damage and condition of all the beams and columns of the critical story (often the ground story). Based on a numerical evaluation of the damage percentages of the vertical (columns) and horizontal (beams) elements, a building can be classified into any of the three damage levels. The buildings presented in this paper were classified as heavily damaged during the exterior evaluation process. As technology advances, there have been recent developments in post-earthquake evaluation methods. One such method requires extensive seismic instrumentation of buildings through rapid analyses of the outputs extracted from sensors [50]. Another one involves the use of machine learning techniques to quickly determine the earthquake-induced building damage using features such as spectral accelerations at a period of 0.3 s, fault distance, building's age, floor area, and the presence of irregularities [51]. In addition to these types of resource-intensive methods that provide in-depth technical information on the impact of earthquakes, an immediate damage assessment method might be more practical to fulfil the urgent requirement to organise earthquake aid and rescue operations. The most practical method is the on-site visual inspection of the earthquake-damaged site. This provides valuable technical information on earthquakes before human interference occurs. This approach was used by our technical team to assess the structural damage to RC buildings in Izmir.

The technical team visited the earthquake-affected locations 10 h after the earthquake to avoid missing any data related to the condition of the buildings during the search and rescue operations. Detailed observations and investigations were performed at collapsed, partially collapsed, and damaged building sites during the four-day stay of the technical team. The findings and evaluations explained in this section are the results of the data and evidence collected during numerous visits to related sites at various times. First, the overall impact of the earthquake is explained, and the findings of site visits are discussed to identify the reasons for the structural damage. With the exception of images from Google Maps, all photographs featured in this section were captured by (and are the properties of) the authors.

4.1. Building inventory and damage statistics in Izmir

In January 2019, the total number of buildings in Izmir was 830,447 [52]. Based on data provided by the Turkish Statistical Institute, almost 70 % of the buildings in Izmir are RC buildings; the remainder are masonry [14]. Residential buildings constitute approximately 90 % of all buildings. Figure 18 shows the distribution of RC buildings in Izmir.

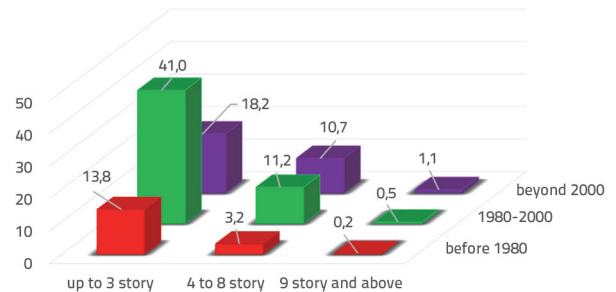


Figure 18. Distribution of RC buildings in Izmir by percentage (adapted from [14])

As depicted in Figure 18, 73 % of the RC buildings have up to three floors, 25 % have four to eight floors, and the remaining (almost 2 %) have nine and more floors. As a group, 70 % of these RC buildings were built before 2000. Two main earthquake codes were in effect at that time: the 1975 and 1998 earthquake codes. Based on the number of years and buildings constructed, it is accurate to state that out of 70 % of the buildings, almost 60 % of them were built according to the rules and regulations of the 1975 Turkish Earthquake Code. Only a few government-approved institutions were permitted to investigate buildings (RC and masonry) at earthquake sites. Table 4 lists the findings of one of these institutions [14, 53]. According to the data, 0.81 % of the buildings experienced moderate-to-major levels of damage, whereas 4.23 % experienced minor damage. The

Table 4. October 20, 2020 dated damage assessment of the buildings in Izmir after the 2020 Aegean Sea earthquake (adapted from [14])

Buildings \ Damage	Collapsed	Demolished	Major damage	Moderate damage	Minor damage	No damage	Total
Number of buildings	50	35	581	688	6.683	150.084	158.121
Percentage of total	0.03	0.02	0.37	0.44	4.23	94.92	100.00

total number of buildings without damage constituted 95 % of the total building inventory. The buildings with major damage and those that collapsed and demolished were all in the Bayraklı District (see Section 4.2).

The distribution of the damage levels of the RC buildings in İzmir is also plotted in Figure 19 as a function of their construction years. As the data indicates, most of the moderate-to-major damage was observed in buildings constructed between 1990 and 2000. Beyond 2010, the damage level shifted towards minor-level damage.

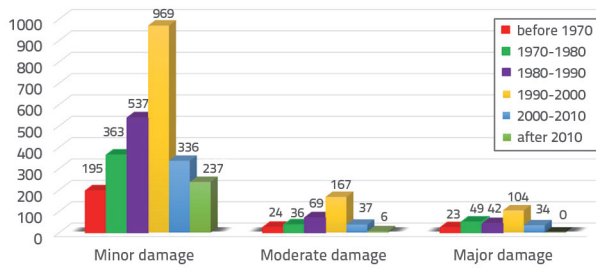


Figure 19. Distribution of damage in İzmir's RC buildings by numbers (adapted from [14])

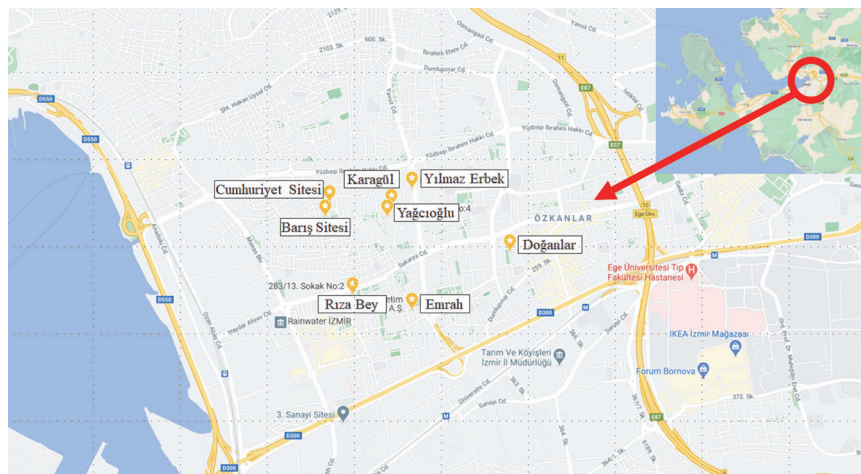


Figure 20. Locations of collapsed buildings in the Bayraklı District

Table 5. General information related to collapsed buildings

Name of apartment	Number of stories	Start of construction	End of construction	Usage	Collapse type
Rıza Bey	9	1993	1994	32 flats and 5 shops	Completely
Doğanlar	8	1990	1992	21 flats and 4 shops	Completely
Emrah	8	1990	1993	28 flats and 6 shops	Completely
Yağcıoğlu Sitesi (2 blocks)	8	1993	-*	14 flats and 4 shops	Block B Completely
Yılmaz Erbek	10	Ends of 1990s	-*	in each block	Partially (half of the building)
Karagül	8	1990s	-*	2 shops	Partially (quarter of the building)
Barış Sitesi (4 blocks)	8	1992	-*	28 flats	Partially (3 Blocks)
Cumhuriyet Sitesi (3 blocks)	8	1990s	-*	-*	Partially (2 Blocks)

* Information could not be obtained.

4.2. Collapsed buildings

As stated in Section 1, the earthquake caused the sudden collapse of 11 RC buildings. Out of these 11 RC buildings, four of them (Rıza Bey, Doğanlar, Emrah, and Block B of Yağcıoğlu Apartment Complex) completely collapsed, and seven of them (Yılmaz Erbek and Karagül Apartments, three blocks in the Barış Apartment Complex and two blocks in the Cumhuriyet Apartment Complex) partially collapsed in the Bayraklı District during the earthquake. All the collapsed buildings had structural framing systems consisting of RC columns and beams. These frames were infilled with brick masonry at all story levels except for the ground story. Most had shops on the ground story which may have produced a weak story at the ground-floor level. General information related to the collapsed buildings is presented in Table 5. The locations of these buildings are shown in Figure 20.

A nine-story building, the Rıza Bey Apartment, collapsed fully during the earthquake. The building construction was completed in 1994. The building consisted of 32 separate apartments and five shops at the ground-story level. Based on videos shot during the collapse, the collapse of this building started with the failure of the ground story columns. After the remainder of the building shifted one story

down, all the other stories began to collapse progressively on top of each other without any translation in the horizontal direction. Photographs of the building before and after the earthquake are shown in Figure 21.

The Doğanlar Apartment Building, with its 21 apartments and four shops at the entrance level, collapsed approximately 1 min after the earthquake. Construction of this eight-story building was completed in 1992. One side of the building was adjacent to the other, with a small gap between them. During its collapse, the Doğanlar Apartment Building shifted away from the adjacent building. Photographs of the buildings before and after the earthquake are shown in Figure 22.



Figure 21. Photographs of the Riza Bey Apartment Building before and after the earthquake



Figure 22. Photographs of the Doğanlar Apartment Building before and after the earthquake



Figure 23. Photographs of the Emrah Apartment Building before and after the earthquake



Figure 24. Photographs of Block B of the Yağcıoğlu Apartment Complex before and after the earthquake



Figure 25. Photographs of the Yılmaz Erbek Apartment Complex before and after the earthquake

Another collapsed building was the eight-story Emrah Apartment Building, completed in 1993. The apartment housed six shops on the ground floor and 28 separate apartments. Photographs of the buildings before and after the earthquake are shown in Figure 23.

Block B of the Yağcıoğlu Apartment Complex collapsed fully after the earthquake, whereas Block A survived the earthquake with heavy damage. Each block of this apartment complex consisted of an 8 story building with 14 separate apartments and four shops located at ground level. Both the buildings were constructed in 1993. Photographs of the buildings before and after the earthquake are shown in Figure 24.

The Yılmaz Erbek Apartment Complex consisted of two adjacent 10-story blocks. The building was constructed in the late 1990s. The ground story level consisted of shops, and the remaining stories comprised separate apartments. The first two stories of one block collapsed during the earthquake. The partially collapsed building was separated from the other buildings, and the total height was reduced. Photographs of the building before and after the earthquake are shown in Figure 25.

The eight-story Karagül Apartment Building, with 28 separate apartments and shops at ground level, was heavily damaged during the earthquake. The building was constructed in the early 1990s. Each residential story consisted of four apartments, and only one-fourth of the building area (corresponding to one apartment) partially collapsed a few minutes after the earthquake. Photographs of the building before and after the earthquake are shown in Figure 26.



Figure 26. Photographs of the Karagül Apartment Building before and after the earthquake

The Barış Apartment Complex, which was comprised of four blocks with eight stories each, was constructed in 1992. Three of these buildings partially collapsed, and one experienced extensive damage without collapse. The first four stories of the two blocks and the first three stories of the other block collapsed on top of each other. The stories over the collapsed portions of the buildings survived the earthquake by leaning towards one side of the buildings. Photographs of the Barış Apartment Complex before and after the earthquake are shown in Figure 27.



Figure 27. Photographs of the Barış Apartment Complex before and after the earthquake

A similar failure mode was observed in the Cumhuriyet Apartment Complex constructed in the early 1990s. The complex consisted of three blocks of eight stories each. One block survived the earthquake with heavy damage; however, the first stories of the other two blocks collapsed, causing the uncollapsed sections of the buildings to shift by one story. Photographs of the Cumhuriyet Apartment Complex before and after the earthquake are shown in Figure 28.



Figure 28. Photographs of the Cumhuriyet Apartment Complex before and after the earthquake

4.3. Severely damaged buildings

There were numerous severely damaged buildings in the city of İzmir during the Aegean Sea earthquake. A typical damage type was diagonal cracking on structural (beams, columns, and shear walls) and non-structural (partition walls) elements, as shown in Figure 29.



Figure 29. Diagonal cracks on structural and non-structural elements

Structural damage to the columns was also significant in some of the buildings, as shown in Figure 30. However, some of the buildings constructed side-by-side were separated because of the collision (hammering effect) of these buildings moving in opposite directions during the earthquake. This type of motion damages the structural elements of buildings. An example of this behaviour is shown in Figure 31.



Figure 30. Severe column damage

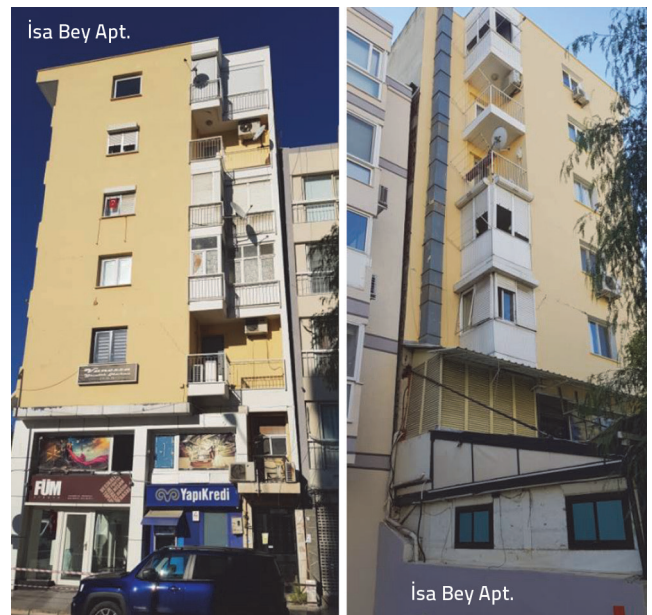


Figure 31. Separated buildings constructed side by side

Table 6. A Comparison of the last four Turkish Earthquake Codes for RC buildings

Description	Turkish Earthquake Codes			
	1975 [55]	1998 [56]	2007 [57]	2018 [41]
Minimum concrete strength [MPa]	No limit*–22,5**	16*–20***	20*	25*
Minimum yield strength of steel [MPa]	Not specified	Not specified	Not specified	420 or greater
Allowed reinforcement bar type	Plain	Plain/Deformed	Deformed	Deformed only
135° stirrup hooks	Yes	Yes	Yes	Yes
Confinement region at ends of beams	Yes	Yes	Yes	Yes
Confinement region at ends of columns	Yes	Yes	Yes	Yes
Strong beams, stronger columns	No	Yes	Yes	Yes

* For all buildings in all earthquake regions; ** Buildings located in the first and second earthquake regions with an importance factor of more than one; *** Buildings located in the first and second earthquake regions with an importance factor of more than one or ductile behaviour

4.4. Evolution of Earthquake Codes in Turkey

The first Turkish Earthquake Code, TEC (1940), [54], was published in 1940 and was originally adapted from the Italian Earthquake Code, which was valid at that time. To date, the code has been modified nine times. The last four versions of this study were published in 1975 [55], 1998 [56], 2007 [57], and 2018. [41].

The partially and fully collapsed RC buildings in this earthquake were constructed in the 1990s (between 1990 and 1998) when the TEC (1975) [55] was in effect. TEC (1975) [55] was considered successful when it was prepared. According to TEC (1975) [55], earthquake loads on buildings were calculated by multiplying the earthquake load coefficient by the seismic weight (calculated using the self-weight and a portion of the live loads) of the building. Factors such as earthquake zones (four zones), building importance factors (two factors), soil types (12 types), fundamental period of the building, design acceleration spectra (four types), and ductility levels of the building (two types) were used to determine this coefficient. Based on this code, the calculated base shear for residential buildings was approximately 8 % to 15 % of the seismic weight of the building. An equivalent lateral static force procedure was used to distribute the total base shear to the story levels. No minimum concrete compressive strength was defined for residential buildings in this code; however, a minimum concrete compressive strength of 22.5 MPa was specified for buildings located in first and second earthquake zones, with an importance factor of more than one. There was no provision related to the type (plain or deformed bars) and minimum yield strength of reinforcing steel bars. The largest sectional forces were known to develop at the beam and column ends. Therefore, provisions related to the confinement of the beam and column ends and the bending stirrup end into the concrete core (135° hooks) were also included in TEC (1975) [55]. Additionally, provisions related to short columns were incorporated into this specification.

Beginning with TEC (1998) [56], a strong beam–stronger column methodology was introduced into the design of RC buildings in Turkey. This required the resisting moment capacities of the connecting columns of a joint to be greater (at least 20 %

than those of the connecting beams of the same joint in the same plane. When a building is subjected to earthquake forces, damage (plastic hinging) occurs first at the bottom ends of the first-story columns. Consequently, plastic hinges will always form at the beam ends if a building is constructed based on the strong beam–stronger column criterion. The collapse of a building requires the formation of hinges at both beam ends, resulting in the highest possible energy absorption capacity before failure. This criterion was also followed in later codes.

Other provisions of TEC (1975) [55], such as the confinement of concrete at the beam and column ends and the bending of stirrups, were explained in more detail in TEC (1998) [56], TEC (2007) [57], and the Turkish Building Earthquake Code [41]. The calculated base shear for residential buildings was approximately 12.5 % to 25 % percent of the seismic weight of the building for these three later codes. A comparison of the last four Turkish earthquake codes for RC buildings is shown in Table 6.

4.5. Evaluation of collapsed and severely damaged buildings

All fully and partially collapsed buildings in this study were designed and constructed before TEC (1998) [56] was implemented. Therefore, the provisions of TEC (1975) [55] will be used to evaluate the design, construction, and behaviour of these buildings during this earthquake. Some collapsed or severely damaged buildings were structurally evaluated for their risk of collapse during earthquakes in recent years (between 2012 and 2018). Corresponding Structural Evaluation Reports (SER hereafter) [58, 59] were prepared and submitted to the inhabitants of these buildings long before the 2020 Aegean Sea earthquake. The information in these SER [58, 59] was also used to evaluate the behaviour of the buildings in this section. A summary of the problems resulting in the damage and collapse is shown in Figure 32. It is important to note that these problems are not only common to RC buildings in Turkey but also to other types of buildings, such as masonry and timber buildings, resulting from past earthquakes that occurred in the region and worldwide [60–62]. The details of these problems are discussed in the following sub-sections.

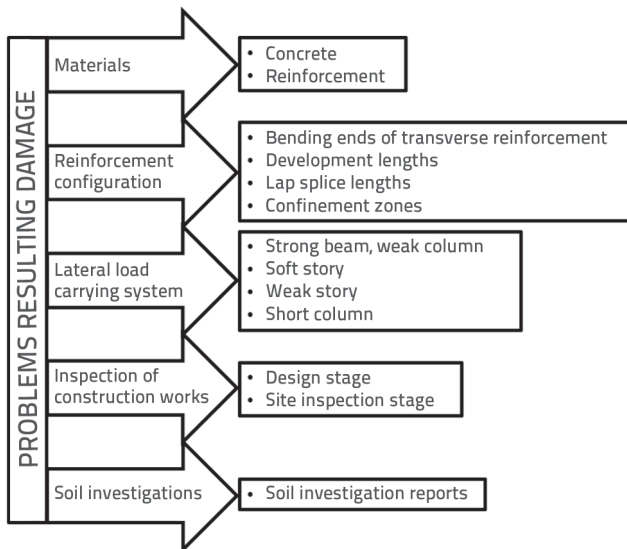


Figure 32. Summary of the problems resulting in damage

4.5.1. Problems related to materials

No minimum concrete compressive strength was specified in TEC (1975) [55] for residential buildings that collapsed during this earthquake. According to the SER, concrete compressive strengths ranging from 10 to 17 MPa was used in the construction of these buildings [58, 59]. These values were determined using ultrasonic and surface-hardness tests performed on the buildings. However, these results should be interpreted with caution because nondestructive testing of concrete compressive strength is unreliable and should be used in combination with the traditional coring technique. The concrete compressive strengths obtained from these tests were lower than those specified in the structural drawings of the buildings.

Based on site observations of the concrete members of the collapsed buildings, it was determined that the concrete used in these buildings consisted of round coarse aggregates of 30–50 mm in diameter. Round and large aggregates would result in poor interlocking behaviour and weak bond strength between the concrete and steel reinforcement. Photographs of some of the concrete samples are shown in Figure 33.



Figure 33. Concrete quality in various collapsed buildings

TEC (1975) [55] did not specify the type of steel reinforcement that should be used in RC buildings. Only plain longitudinal and transverse reinforcing bars were available in Turkey during the early 1990s. The steel-reinforcing bars exhibited a minimum yield strength of 220 MPa. Deformed reinforcing bars have been available since the mid-1990s. Visual observations of the collapsed buildings confirmed that combinations of these reinforcements were used during construction. For example, plain bars were used in the construction of the Emrah Apartment, both as longitudinal and transverse reinforcements. The longitudinal and transverse reinforcements used in the Rıza Bey Apartment were deformed and plain, respectively. In the Yılmaz Erbek Apartment, only deformed bars were used as reinforcement. Photographs of the reinforcements are shown in Figure 34.



Figure 34. Reinforcement types in various collapsed buildings

Most of the buildings in the area had moisture problems owing to the humid climate, high water table level, and insufficient water insulation, particularly at the ground level. Therefore, the reinforcements of the structural members of these buildings corroded extensively, resulting in a significant reduction in the cross-sectional area of the reinforcements. Examples of the corroded reinforcements are shown in Figure 35. It is important to note that these mistakes are repeated when building damage is investigated during most earthquakes. For instance, the field observations recorded after the Sivrice, Elazığ, Turkey earthquake on 24 January 2020 are an example of this [63].



Figure 35. Corrosion of reinforcements due to moisture

4.5.2. Problems related to reinforcement configuration

As stated previously, TEC (1975) [55] required closely spaced stirrups (confinements) to be used at the end regions (confinement zones) of the beams and columns. The length of this region was a minimum of one-sixth of the column height, or 450 mm for the columns. TEC (1975) [55] also specified the maximum distance between the two stirrups in this region as 100 mm. Site observations indicated that no confinement was used at the ends of the beams and columns. Examples of the reinforcement configurations of the columns and beams of collapsed buildings are shown in Figure 36. This finding was also supported by various SER [58, 59] prepared for these collapsed buildings.



Figure 36. Reinforcement configurations of the columns and beams of the collapsed buildings

Although TEC (1975) [55] required bending the ends of the stirrups into the concrete core (135° hooks), the ends of the stirrups were only bent by 90°, resulting in the opening of the stirrups after the spalling of the cover concrete in the beams and columns. Photographs of

these stirrups in various collapsed buildings are shown in Figure 37. As with the observations made in the materials section, problems related to the reinforcement configuration have been frequently observed in Turkey following an earthquake.

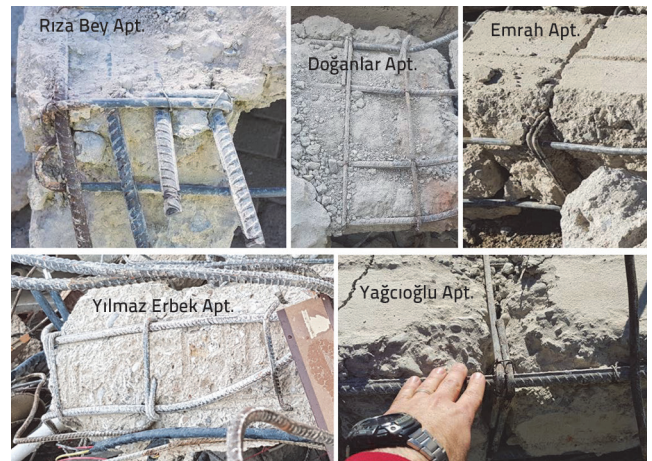


Figure 37. Ends of the stirrups (bent 90°) of the collapsed buildings

4.5.3. Problems related to the lateral load carrying systems

TEC (1975) [55] did not define irregularities based on story stiffness. The effects of this type of irregularity were first introduced into the 1998 earthquake code [56]. The strong beam–stronger column requirement first appeared in TEC (1998) [56]. The first few stories of some of the buildings collapsed like a sandwich during the earthquake. These buildings had story stiffness irregularities at the ground-story level which likely played a major role in their collapse. Photographs of these buildings are shown in Figure 38.



Figure 38. Collapsed buildings due to the failure of first story columns

According to TEC (1975) [55], the transverse reinforcement was confined along the length of the short columns. An example of the damage caused to short columns after the earthquake is shown in Figure 39. Reinforcement confinement was not observed in the short columns.



Figure 39. Short column formation in a severely damaged building

4.5.4. Problems related to inspection of construction works

Before the beginning of the millennium, construction work in Turkey had not been properly inspected. Reports related to soil investigations and structural designs were not always reviewed by an institution. During construction, the strength of the materials (concrete and steel) used was not tested, and the correct application of the structural drawings in terms of the reinforcement configuration and dimensions of the structural members was not confirmed. In some collapsed and severely damaged buildings, the SER prepared before the earthquake indicated that the reinforcement configuration of the structural drawings differed from that of the constructed buildings. Furthermore, the sizes of the constructed structural members did not match those in the structural drawings of some buildings [58, 59]. For example, a column of 250 × 800 mm in size in structural drawings was constructed in 1988 as 250 × 500 mm along the height of a 9-story building.



Figure 40. Beam damaged for plumbing (Karşıyaka, İzmir)

The inspection mechanism before (the design stage) and during the construction process changed significantly during the 2000s. After the earthquake, the conditions of numerous damaged buildings

in İzmir were investigated by experts from the Turkish Ministry of the Environment and Urbanization. Based on their findings, some buildings were determined to be unsafe for occupants and were either demolished immediately or designated for repair and/or strengthening. During this post-earthquake assessment process, we observed that the structural members of some buildings were damaged or destroyed for various reasons before the earthquake. Examples of this type of damage and destruction are shown in Figure 40. The bottom longitudinal reinforcement of the basement beam shown in this figure was cut at midspan, and the top longitudinal reinforcement was damaged at the support region to instal utility pipes inside the building. The stirrups were also cut from the damaged sections.

4.5.5. Problems related to soil investigation

In Turkey, early geotechnical site studies were initiated in 1986 as part of the requirements for zoning plans [63]. However, it was not until two major earthquakes occurred, the Kocaeli Earthquake in August 1999 and the Düzce Earthquake in November 1999, that the existing law was amended to require geological site reports as part of the building permit acquisition process [64]. Because of problems regarding the content of the geotechnical reports, the government intervened and furnished the details of a typical site report. As part of these efforts, in January 2000, the Ministry of Public Works issued a memorandum to make geotechnical site reports a structural design requirement. As the historical evolution of geotechnical site reports in Turkey suggests, soil-associated structural design parameters were not prioritised until the early 2000s. This underscores the problems in buildings constructed before 2000. Most likely, this problem played a significant role in the buildings that collapsed and experienced moderate-to-major damage in Bayraklı District [7, 11].

5. Conclusions

The following conclusions can be drawn based on the technical team's site observations:

- Local soil class (site effect) is an important parameter that should be incorporated into earthquake analysis and building design. The buildings in Bayraklı suffered mostly from this phenomenon. Therefore, thorough earthquake analyses should be performed for all existing buildings in the area.
- TBEC (2018) [41] requires a site-specific elastic acceleration spectrum only for local soil class ZF. Although the code allows design engineers to request similar studies for other soil classes, there is no clear justification for this request. Thus, adding a statement to the code requiring a site-specific elastic acceleration spectrum in areas like Bayraklı would help satisfy earthquake design requirements.
- To prevent any further loss of life and property during future earthquakes, a detailed earthquake hazard assessment should be prepared, specifically for buildings located in the İzmir Bay area.

- The fully and partially collapsed buildings in İzmir during the Aegean Sea earthquake were constructed when TEC (1975) [55] was in effect. However, many requirements in the code were not followed during the design or construction stages.
- Inspections during the design and construction phases were not properly performed for buildings constructed before

2000. Therefore, all RC buildings constructed in Turkey before 2000 should be re-evaluated for their structural performance.

- Administrative precautions should be taken to sustain the structural integrity of RC buildings during their lifespan.

REFERENCES

- [1] Sahin, B.E., Tunc, G., Ozsarac, E.: Disaster Management and Public-Private Partnership in Turkey, International Civil Engineering and Architecture Conference, ICEARC19, Trabzon, Turkey, 17-20 April 2019.
- [2] Aral, M., Tunc, G.: A Proposal for the Establishment of Building Identity Numbers in Turkey Based on the Performance of Buildings During Earthquakes, *Journal of Disaster and Risk*, 4 (2021) 1, pp. 20-41.
- [3] MTA (General Directorate of Mineral Research and Exploration), <https://www.mta.gov.tr/v3.0/hizmetler/yenilenmis-diri-fay-haritalari>, 01.04.2022 (in Turkish).
- [4] AFAD (Disaster and Emergency Management Authority): Preliminary evaluation report of October 30, 2020 Mw 6.6 Aegean Sea, Seferihisar (İzmir) Earthquake. Turkish Ministry of Interior, Department of Earthquake, Ankara, Turkey, 2020 (in Turkish).
- [5] TÜİK (The Turkish Statistical Institute), <https://www.tuik.gov.tr/>, 01.04.2022 (in Turkish).
- [6] AA (Anadolu Agency), <https://www.aa.com.tr/tr/turkiye/bakan-kurum-izmirde-tum-hasar-tespit-calismalar-tamamlandi/2039895>, 01.04.2022 (in Turkish).
- [7] Nuhoglu, A., Eren, M.F., Hizal, Ç., Kincal, C., Erdoğan, D.Ş., Özdağ, Ö.C., Akgün, M., Ercan, E., Kalfa, E., Köksal, D., İpek, Y., Sezer, A.: A reconnaissance study in Izmir (Bornova Plain) affected by October 30, 2020 Samos earthquake, *International Journal of Disaster Risk Reduction*, 63 (2021), 102465, doi: 10.1016/j.ijdr.2021.102465
- [8] Cetin, K.O., Altun, S., Askan, A., Akgün, M., Sezer, A., Kincal, C., Özdağ, Ö.C., İpek, Y., Unutmaz, B., Gülerce, Z., Özacar, A., Ilgaç, M., Can, G., Cakir, E., Söylemez, B., El-Sayeed, A., Zazour, M., Bozyiğit, İ., Tuna, Ç., Köksal, D., Karimzadeh, S., Uzel, B., Karaali, E.: The site effects in Izmir Bay of October 30 2020, M7.0 Samos Earthquake, *Soil Dynamics and Earthquake Engineering*, 152 (2022), 107051, doi: 10.1016/j.soildyn.2021.107051
- [9] Akinci, A., Cheloni, D., Dindar, A.A.: The 30 October 2020, M7.0 Samos Island (Eastern Aegean Sea) Earthquake: effects of source rupture, path and local-site conditions on the observed and simulated ground motions, *Bulletin of Earthquake Engineering*, 19 (2021), pp. 4745-4771, doi: 10.1007/s10518-021-01146-5
- [10] Makra, K., Rovithis, E., Riga, E., Raptakis, D., Ptilakis, K.: Amplification features and observed damages in Izmir (Turkey) due to 2020 Samos (Aegean Sea) earthquake: identifying basin effects and design requirements, *Bulletin of Earthquake Engineering* 19 (2021), pp. 4773-4804, doi: 10.1007/s10518-021-01148-3
- [11] Demirci, H.E., Karaman, M., Bhattacharya, S.: A survey of damage observed in Izmir due to 2020 Samos-Izmir earthquake, *Natural Hazards*, 111 (2022), pp. 1047-1064, doi: 10.1007/s11069-021-05085-x
- [12] Binici, B., Yakut, A., Canbay, E., Akpınar, U., Tuncay, K.: Identifying buildings with high collapse risk based on samos earthquake damage inventory in Izmir, *Bulletin of Earthquake Engineering*, 20 (2022), pp. 7853-7872, doi: 10.1007/s10518-021-01289-5
- [13] Demir, A., Altıok, T.Y.: Numerical assessment of a slender structure damaged during October 30, 2020, Izmir earthquake in Turkey, *Bulletin of Earthquake Engineering*, 19 (2021), pp. 5871-5896, doi: 10.1007/s10518-021-01197-8
- [14] Yakut, A., Sucuoğlu, H., Binici, B., Canbay, E., Donmez, C., İlki, A., Caner, A., Celik, O.C., Ay, B.Ö.: Performance of structures in Izmir after the Samos island earthquake, *Bulletin of Earthquake Engineering*, 20 (2022), pp. 7793-7818, doi: 10.1007/s10518-021-01226-6
- [15] EON-Global Catastrophe Recap: November 2020, http://thoughtleadership.aon.com/Documents/20201210_analytics-if-november-global-recap.pdf, 01.04.2022.
- [16] Okay, A.I., Zattin, M., Cavazza, W.: Apatite fissiontrack data for the Miocene Arabia-Eurasia collision, *Geology*, 38 (2010), pp. 35-38.
- [17] Kuruoğlu, M., Eskisar, T.: Effect of local soil conditions on dynamic ground response in the southern coast of Izmir Bay, Turkey, *Russian Geology and Geophysics*, 56 (2015), pp. 1201-1212.
- [18] Drahor, M.G., Berge, M.A.: Integrated geophysical investigations in a fault zone located on southwestern part of Izmir city, Western Anatolia, Turkey, *Journal of Applied Geophysics*, 136 (2017), pp. 114-133.
- [19] Emre, Ö., Barka, A.: Active faults between Gediz Graben and Aegean Sea (İzmir Region), *Earthquake Symposium for Western Anatolia, Izmir, Turkey*, (2000), pp. 131-132 (in Turkish).
- [20] Ocakoğlu, N., Demirbağ, E., Kuşçu, İ.: Neotectonic structures in the area offshore of Alaçatı, Doğanbey and Kuşadası (western Turkey): Evidence of strike-slip faulting in the Aegean extensional province, *Tectonophysics*, 391 (2004), pp. 67-83.
- [21] Ocakoğlu, N., Demirbağ, E., Kuşçu, İ.: Neotectonic structures in Izmir Gulf and surrounding regions (western Turkey): Evidences of strike-slip faulting with compression in the Aegean extensional regime, *Marine Geology* 219 (2005), pp. 155-171.
- [22] Emre, Ö., Özalp, S., Doğan, A., Özaksoy, V., Yıldırım, C., Göktaş, F.: Active faults in the vicinity of Izmir and their earthquake potential, Report No: 10754, General Directorate of Mineral Research and Exploration, Ankara, Turkey, 2005 (in Turkish).
- [23] Altun, S., Sezer, A., Göktepe, A.B.: A preliminary microzonation study on Northern Coasts of Izmir: Investigation of the local soil conditions, *Soil Dynamics and Earthquake Engineering*, 39 (2012), pp. 37-49.
- [24] Ketin, İ.: Türkiye'nin genel tektonik durumu ile baslıca deprem bölgeleri arasındaki ilişkiler, *Bulletin of Mineral Research and Exploration*, 71 (1969), pp. 129-134 (in Turkish).
- [25] Bozkurt, E.: Neotectonics of Turkey - A Synthesis, *Geodinamica Acta*, 14 (2001), pp. 3-30.
- [26] Aksu, A.E., Piper, D.J.W., Konuk, T.: Late Quaternary tectonic and sedimentary history of outer Izmir and Candarli bays, Western Turkey, *Marine Geology*, 76 (1987), pp. 89-104.

- [27] Sozibilir, H., Uzel, B., Sumer, O., Inci, U., Ersoy, E., Kocer, T., Demirtas, R., Ozkaymak, C.: Data about coordinated working of the E-W oriented İzmir Fault and the NE-SW oriented Seferihisar Fault: Kinematical and paleoseismological studies on active faults occurring gulf of İzmir, Western Anatolia, *Bulletin of Turkish Geology*, 52 (2008), pp. 91-114 (in Turkish).
- [28] Sozibilir, H., Sumer, O., Uzel, B., Ersoy, E., Erkul, F., Inci, U., Helvacı, C., Ozkaymak, C.: Seismic geomorphology of October 17–20, 2005 Sigacık Bay earthquakes and relation with stress areas in region, Western Anatolia, *Bulletin of Turkish Geology*, 53 (2009), pp. 217-238 (in Turkish).
- [29] Uzel, B., Sozibilir, H., Ozkaymak, C.: Evolution of an actively growing superimposed basin in Western Anatolia: The Inner Bay of İzmir, *Turkish Journal of Earth Sciences*, 21 (2012), pp. 439-471.
- [30] Kincal, C.: Evaluation of geological units in İzmir inner bay and its vicinity by using GIS and remote sensing systems in terms of engineering geology, PhD Thesis, Dokuz Eylül University, 2004 (in Turkish).
- [31] Pamuk, E., Özdağ, Ö.C., Akgün, M.: Soil characterization of Bornova Plain (İzmir, Turkey) and its surroundings using a combined survey of MASW and ReMi methods and Nakamura's (HVSr) technique, *Bulletin of Engineering Geology and the Environment*, 78 (2019), pp. 3023-3035.
- [32] AFAD (Disaster and Emergency Management Authority), Turkish Ministry of Interior, Ankara, <https://tdth.afad.gov.tr/>, 01.04.2022 (in Turkish).
- [33] MTA (General Directorate of Mineral Research and Exploration), <http://yerbilimleri.mta.gov.tr/anasayfa.aspx>, 01.04.2022 (in Turkish).
- [34] Pamuk, E., Akgün, M., Özdağ, Ö.C., Gönenç, T.: 2D soil and engineering-seismic bedrock modeling of eastern part of İzmir inner bay/Turkey, *Journal of Applied Geophysics*, 137 (2017), pp. 104-117.
- [35] KOERI (Kandilli Observatory and Earthquake Research Institute): October 30, 2020 Aegean Sea Earthquake Press Bulletin, Boğaziçi University, İstanbul, Turkey, 2020 (in Turkish).
- [36] USGS (The United States Geological Survey) <https://earthquake.usgs.gov/earthquakes/eventpage/us7000c7y0/executive>, 01.04.2022.
- [37] CMT (Harvard), <https://www.globalcmt.org/>, 01.04.2022.
- [38] GFZ, <https://geofon.gfz-potsdam.de/>, 01.04.2022.
- [39] METU (Middle East Technical University): Seismic and structural damages related to site observations for the October 30, 2020 Samos Island (off the coast of Seferihisar, İzmir) Earthquake, Report No: ODTÜ/DMAM 2020-03, Ankara, 2017 (in Turkish).
- [40] MTA (General Directorate of Mineral Research and Exploration): Field Observations and Evaluation Report of October 30, 2020 (Mw=6.6) Aegean Sea Earthquake, Turkish Ministry of Energy and Mineral Resources, Ankara, Turkey, 2020 (in Turkish).
- [41] Ministry of Environment and Urban Planning: Turkish Building Earthquake Code (TBEC), Ankara, Turkey, 2018 (in Turkish).
- [42] AFAD (Disaster and Emergency Management Authority): Turkish Ministry of Interior, Ankara, Turkey <https://depem.afad.gov.tr/istasyonlar>, 01.04.2022 (in Turkish).
- [43] Grünthal, G.: European Macroseismic Scale, *Cahiers du Centre Européen de Géodynamique et de Séismologie*, 15 (1998) (in French).
- [44] GNDT-SSN, Gruppo Nazionale per la Difesa dai Terremoti, Scheda di esposizione e vulnerabilità e di rilevamento danni di primo livello e secondo livello (muratura e cemento armato), Gruppo Nazionale per la Difesa dai Terremoti: Roma, Italy, 1994, (in Italian).
- [45] Applied Technology Council (ATC) ATC-20 Procedures for Post-Earthquake Building Safety Evaluation Procedures. Redwood, CA: Applied Technology Council, 1995.
- [46] Anagnostopoulos, S.A., Moretti, M., Panoutsopoulou, M., Panagiotopoulou, D., Thoma, T.: Post earthquake damage and usability assessment of buildings: Further development and applications, Final report, European Commission - D.G. Environment, Civil Protection - EPPO, 2004.
- [47] Anagnostopoulos, S., Moretti M.: Post-earthquake emergency assessment of building damage, safety and usability - Part 2: Organisation, Soil Dynamics and Earthquake Engineering. 28 (2008), 3, pp. 233-244, doi: 10.1016/j.soildyn.2006.05.008
- [48] Uroš, M., Šavor Novak, M., Atalič, J., Sigmund, Z., Baniček, M., Demšič, M., Hak, S.: Post-earthquake damage assessment of buildings – procedure for conducting building inspections, *GRAĐEVINAR*, 72 (2020) 12, pp. 1089-1115, doi: 10.14256/JCE.2969.2020
- [49] Turkish Chamber of Civil Engineers: Damage Evaluation of Reinforced Concrete and Masonry Buildings Affected by Earthquake, Ankara, Turkey, 72 p., 2016 (in Turkish).
- [50] Naeim, F., Lee, H., Hagie, S., Bhatia, H., Alimoradi, A., Miranda, E.: Three-dimensional analysis, real-time visualization, and automated post-earthquake damage assessment of buildings, *Structural Design of Tall and Special Buildings*. 15 (2006), 1, pp. 105-138, doi: 10.1002/tal.345
- [51] Mangalathu, S., Nweke, C.C., Yi, Z., Burton, H.V., Sun, H.: Classifying earthquake damage to buildings using machine learning, *Earthquake Spectra*, 36 (2020), 1, pp. 183-208, doi: 10.1177/8755293019878137
- [52] Metropolitan Municipality of İzmir, İzmir City Guide Building Count Distribution Map, <https://kentrehberi.izmir.bel.tr/izmirkentrehberi#>, 01.04.2022 (in Turkish).
- [53] METU, The Samos (İzmir-Seferihisar Offshore) Earthquake [30 October 2020 Mw=6.6] Field Observations On Seismic and Structural Damage, Earthquake Engineering Research Center, Middle East Technical University, Report No: METU/EERC 2020-03, November 2020.
- [54] Ministry of Public Works and Settlement: Italian building instructions in earthquake districts (TEC), Ankara, Turkey, 1940 (in Turkish).
- [55] Ministry of Public Works and Settlement: Specification for structures to be constructed in disaster areas (TEC), Ankara, Turkey, 1975 (in Turkish).
- [56] Ministry of Public Works and Settlement: Specification for structures to be constructed in disaster areas (TEC), Ankara, Turkey, 1998 (in Turkish).
- [57] Ministry of Public Works and Settlement: Specification for buildings to be constructed in earthquake areas (TEC), Ankara, Turkey, 2007 (in Turkish).
- [58] Bayraklı Municipality, Earthquake Investigation Center, İzmir, Turkey, <https://bayrakli.bel.tr/Sayfa/80/depem-etud-merkezi-baydem>, 01.04.2022 (in Turkish).

- [59] AA (Anadolu Agency) Ankara, Turkey, <https://www.aa.com.tr/tr/turkiye/bayrakli-belediye-baskani-sandaldan-rizabey-ve-doganlar-apartmanlari-raporuyla-ilgili-aciklama/2030535,01.04.2022> (in Turkish).
- [60] Radnić, J., Grgić, N., Buzov, A., Banović, I., Smilović Zulim, M., Baloević, G., Sunara, M.: Mw 6.4 Petrinja earthquake in Croatia: Main earthquake parameters, impact on buildings and recommendation for their structural strengthening, *GRAĐEVINAR*, 73 (2021), 11, pp. 1109-1128, doi: 10.14256/JCE.3243.2021
- [61] Mertol, H.C., Tunc, G., Akis, T.: Evaluation of masonry buildings and mosques after Sivrice earthquake, *GRAĐEVINAR*, 73 (2021), 9, pp. 881-892, doi: 10.14256/JCE.3101.2021
- [62] Šavor Novak, M., Uroš, M., Atalić, J., Herak, M., Demšić, M., Baniček, M., Lazarević, D., Bijelić, N., Crnogorac, M., Todorčić, M.: Zagreb earthquake of 22 March 2020 – preliminary report on seismologic aspects and damage to buildings, *GRAĐEVINAR*, 72 (2020), 10, pp. 843-867, doi: 10.14256/JCE.2966.2020
- [63] Mertol, H.C., Tunc, G., Akis, T.: Damage Observation of Reinforced Concrete Buildings after 2020 Sivrice (Elazığ) Earthquake, Turkey, *Journal of Performance of Constructed Facilities*, 35 (2021), 5, 04021053, doi: 10.1061/(ASCE)CF.1943-5509.0001619
- [64] Karakus, K: Geological soil reports and legal regulations. Ankara, Turkey: Chamber of Geological Engineers, 2009.